ADVANCES IN TAILINGS DAM BREACH MODELLING AND CREDIBLE FAILURE MODE OUTCOME IN TAILINGS DAM BREACH ASSESSMENT USING THE MATERIAL POINT METHOD

Marcelo Llano-Serna[1], Scott H Lines[1], Nicolas Pereira[1], Seyedmohammadjavad Seyedan[2], Sudheer Prabhu[1] and Mike Liu[1]

[1] Red Earth Engineering, a Geosyntec Company; [2] Geosyntec Finland

https://doi.org/10.56295/AGJ6045

ABSTRACT

Recent tailings dam failures underscore the need for better tools to understand and mitigate the potential impacts of such events. The Global Industry Standard on Tailings Management (GISTM), introduced in response to catastrophic tailings dam failures, is an aspirational standard that defines credible failure modes as technically feasible failure mechanisms. This is an excellent first step, however, GISTM does not state which methodology to assess these failure modes. A commonly employed approach that would be considered as industry standard is the Failure Modes and Effects Analysis (FMEA). The FMEA applies rigour to decision making but is still subject to subjectivity, relying on engineering judgement to inform risk. A tool that can be utilised to understand tailings dam failure further and supplement the FMEA process is the Material Point Method (MPM). A numerical method which allows for large strain, as required in breach analysis, with commonly accepted constitutive soil models and relatively limited computational power requirements in comparison to alternative large strain modelling methodologies. Six case studies utilising MPM is presented. The case studies incorporate an array of tailings facility design, location, complexity, lifecycle and regulatory environments, demonstrating how MPM can enhance understanding of the complex challenges. The benefits of utilising MPM with existing guidelines and current industry practices is highlighted, providing lessons learned and recommendations for implementation of MPM into projects. MPM is a tool that can reduce risk and promote better-informed decision-making, furthering the GISTM goal of 'zero harm to people and the environment with zero tolerance for human fatality.'

1 INTRODUCTION

Leaders in the tailings storage facility (TSF) industry recently recognised two interpretations of credible failure modes. The first is on whether the potential failure mode is possible and the second is rooted in the determination that the probability of the failure mode is considered non-negligible (Small et al., 2023). Although GISTM (2020) highlights that the term credible failure mode is not associated with a probability of an event occurring, Martens and Kupper (2024) remark that GISTM intended to emphasise that the existence of credible failure modes is not related to the facility because acknowledging a credible failure mode is not a statement of whether its probability is high or low. ANCOLD (2022) and CDA (2007) recommend conceptually connecting failure modes to unwanted consequences (e.g. the catastrophic failure of a TSF embankment) using bow-tie diagrams and assessing risk using tools such as Failure Mode and Effects Analysis (FMEA). The outcomes of these assessments are diagrams and results are qualitative and require the output of technical assessments, such as Tailings Dam Breach Assessments (TDBA), to determine the potential consequence of hypothetical failure events. CDA (2021) recommends that selected scenarios when undertaking TDBA should consider critical and credible failure mechanisms. Although the recent technical literature highlights the role of credibility in failure mode selection, the reliability of modelling credible consequences remains relatively unexplored.

This paper describes how recent advances in computational mechanics have resulted in adopting methodologies such as the Material Point Method (MPM) to improve the reliability of modelled failure modes. Background of MPM is provided, leading into four forensic studies that investigate the failure of a TSF and six industry projects ranging from a simple column collapse to a more complicated multi-plane failure surface. The extensive presentation of case studies is used to communicate the available scenarios that benefit from MPM, the core link between them is that the potential for large strain to occur is present. These scenarios are then expanded further to outline available solids content, rheological behaviour and the various methodologies that produce volume estimates. This comprehensive review of the state of MPM within the tailings industry has been designed to provide guidance in most of the relevant areas for practitioners seeking to utilise MPM within their projects.

2 MPM IN THE CONTEXT OF TDBA

The Canadian Dam Association technical bulletin on TDBAs (CDA, 2021) is one of the more recent guidelines published to inform dam safety professionals. CDA (2021) constituted a step forward, highlighting, among other key factors, the complex non-Newtonian flow behaviour exhibited by tailings. A common misconception in the industry assumes that when tailings are modelled to behave like water (Newtonian), it results in conservative consequence estimates (Llano-Serna, 2023). This assumption can be correct in certain scenarios since Newtonian behaviour results in over predicting the inundation areas (i.e., water flow will cover a larger area than mudflow). However, in other scenarios it is incorrect as the assumption of Newtonian behaviour under predicts mudflow depths, particularly near the dam toe, where mining/processing plant infrastructure is usually located. Newtonian flows can also under predict lateral spread perpendicular to the direction of the advancing plume. Larger deposition depths seen in non-Newtonian flows have the potential to flow perpendicular to the flow direction near the embankment toe. These misunderstandings can result in inadequate risk mitigation measures and mischaracterisation of risk profiles because the models used produce non-credible outcomes. Tailings, especially those contained at high solids concentration, do not behave like water (CDA, 2021).

Numerous factors and failure modes can cause tailings dam failure. One example includes tailings liquefaction, which has been demonstrated to have played a significant role in recent dam failures like Cadia in Australia or Fundão and Brumadinho in Brazil. The International Commission on Large Dams bulletin 194 (ICOLD, 2023) recommends following NASEM (2021) for guidance on state-of-practice guidelines to assess earthquake-induced soil liquefaction and its consequences. NASEM highlights the emergence of techniques such as MPM to predict liquefaction and its consequences. Additionally, the United States Society on Dams (USSD, 2022) highlighted MPM as one of the promising methods for modelling the deformation of embankment dams.

2.1 MATERIAL POINT METHOD

MPM was developed in the 1990s (Sulski et al. 1994, 1995) to address the limitations of traditional mesh-based modelling methods (e.g., Finite Element Method). MPM combines the strengths of both particle and mesh-based methods, allowing it to conduct large-strain calculations. MPM is based on continuum mechanics, and its algorithm ensures the conservation of mass and momentum in calculations. In each timestep, MPM uses a mesh to solve the equation for the conservation of momentum. The MPM algorithm saves time-dependent data in material points and resets the mesh, preventing the primary limitation of mesh-based methods. The algorithms can update stress at the beginning or end of each calculation cycle. Wallstedt and Guilkey (2008) showed that updating stress at the end is more efficient.

Explicit MPM algorithms that use simple linear functions can result in numerical errors caused by cell crossing (Sulski et al. 1994). Bardenhagen and Kober (2004) introduced the Generalized Interpolation Material Point (GIMP) to mitigate cell crossing errors and improve stability. GIMP has two main versions: uGIMP, where material point domains remain unchanged, and cpGIMP, which tracks changes within domains. Despite improvements, GIMP faces challenges to model shear deformation, tensile loading fractures, and modelling curved geometries (Sołowski et al., 2021). Sadeghirad et al. (2011) introduced the Convected Particle Domain Interpolation (CPDI) for better handling curved geometries and shear deformation. Most MPM algorithms use explicit and implicit time integration schemes (Sołowski et al., 2021), with explicit methods being much more common and it is the main focus of this work.

MPM-based tools have advantages and disadvantages that should be carefully considered. The continuum mechanics nature of MPM means that methods based on it can use common models (e.g., Mohr-Coulomb) as well as more advanced models (e.g., Nor-Sand and P2P-Sand) for capturing particle-to-particle and particle-to-fluid interactions in tailings materials. While ongoing developments of MPM are continuously improving its versatility and usability, many MPM tools are research-based and lack the robustness and support of commercial geotechnical software (i.e., FLAC or Plaxis). Most MPM tools do not incorporate the ability to replicate construction stages, making it difficult to capture instability triggers. Engineering judgment can help overcome these challenges, however it introduces subjectivity into the process.

2.1.1 Computational effort

Computational effort continues to be a key challenge for MPM. As opposed to something like the limit equilibrium method (LEM), commonly used in stability assessments. MPM is more similar to FEM or FDM methods, though potentially with slightly higher computational effort required. Over time this computational effort has decreased significantly and with more computational power being made available and the development of more powerful MPM engines this is expected to continue to decrease. Despite the extra computational effort required, the advantages of adopting MPM modelling for TDBA are significant. Being able to produce more realistic and reliable results is invaluable for assessing the potential consequences and risk of a facility. The limitations in computational effort may be mitigated with appropriate planning during the design stages and adequate modelling simplifications.

2.1.2 Software packages and tools

The modelling team has experience with the MPM engines listed in this Section. This list is not exhaustive and there are many other MPM engines available.

ANURA3D (Anura3D MPM Research Community, 2025) is the most widely known and used MPM engine. The modelling community using this tool is relatively extensive, and new users can engage the community for assistance. Anura is recommended for new MPM users due to its ease of use and low learning curve. Anura is an open-source software and available for free. Nevertheless, Anura requires a commercial pre-processing tool called GiD. The pre-processing tool brings many advantages, such as the graphic user interface (GUI), allowing modellers to define boundary condition problems without significant coding. Anura has an active community and is well documented with a manual and tutorials. The latest version of Anura has some parallelisation capabilities and Anura3D community are further improving the parallelisation of the software so it can do 3D and big 2D models in an effective and timely manner. In addition, the 2025 version of Anura3D includes stage construction ability which improves the modelling accuracy.

CB-Geo (Kumar et al., 2019) is an open-source tool for MPM simulations supporting various constitutive, multiple stress update and velocity update strategies. It is the one of the most efficient available implementations of MPM to date, supporting parallel processing and clusters computing. However, it currently only runs using Linux, it is not thoroughly documented and its development and communities are no longer active.

MPAC (Purvance and Coetzee, 2024) is the soon to be released code developed by the ITASCA Consulting Group (ITASCA) who are responsible for the widely used FLAC and PFC (Llano-Serna et al., 2024). This is a closed-sourced commercial software but will have the technical support available for users and run within the FLAC environment. So, users familiar with FLAC will have a gentler learning curve then some of the other options presented here.

MPMPUC-Rio (Fernandez, 2020) is a numerical simulator based on MPM that supports several constitutive relationships and coupled hydro-mechanical modelling. It incorporates multiprocessor memory parallelisation techniques that allow simulations of many material points, allowing for 3D models and large 2D models to be solved efficiently. However, it is closed source, command-based and lacks documentation and examples, so it is not as user-friendly. Additionally, the critical time step is limited to a fixed value that requires manual adjustment, so the efficiency of the calculation can vary greatly. The program is currently only available at the author's discretion.

Uintah-MPM (Guilkey et al., 2009) was developed at the University of Utah in 1997. Uintah provides a computational framework that includes modelling software components and libraries, including an MPM component. The MPM component of Uintah supports advanced parallelisation of processors, 2D and 3D modelling, and various constitutive models, including important geotechnical models. Uintah's open-source nature lets developers access and modify the code as needed. It also offers various time-stepping algorithms, simplifying its use. Nevertheless, the lack of a graphical interface for creating geometries makes working with the software challenging.

2.2 HISTORICAL BENCHMARKING AND FORENSIC STUDIES

Zabala (2010) simulated the failure of the Aznalcóllar dam using MPM to build the model using 15 construction stages and incorporating the brittle clay foundation characterised by means of a strain-softening Mohr-Coulomb elasto-plastic model. The model could predict the development of a localised shear band at the toe and the subsequent progressive failure with the modelled failure matching actual field observations (Figure 1). In the analysis performed no prior assumptions were made about the location, shape or depth of the failure surface.

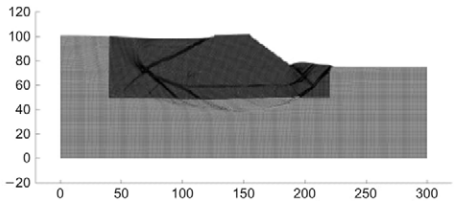

Figure 1: MPM model after tailings liquefaction, horizontal and vertical axis are expressed in metres (Zabala and Alonso, 2010)

Pierce (2021) examined the 2018 Cadia tailings dam failure, located in New South Wales, Australia. The initial and final field topography, overlaid with the MPM results is shown in Figure 2. The MPM results provide an excellent match with the final field topography, with the Pump House location from the model being within 10 m of the observed Pump House location. The model was constructed using a fully coupled hydromechanical MPM formulation for saturated materials, with the material above the water table assumed to be dry. Mohr-Coulomb was applied to the material with an undrained strength assigned for the liquefied tailings.

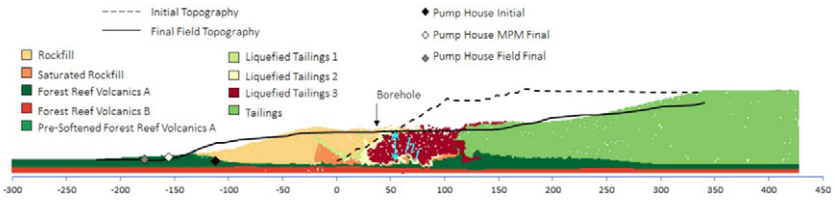

Figure 2: Cadia - MPM versus the pre and post-failure topography (modified from Pierce 2021)

An additional study utilising MPM was the Expert Panel investigation of the failure of Feijão Dam I (Robertson et al., 2019 Appendix H). This case resulted in a significant mudflow that travelled rapidly downstream with failure occurring in the space of 10 seconds and resulting in approximately 9.7 million cubic metres of tailings flowing out of the facility. MPM was able to simulate the first 15 seconds of failure with velocity ranging from 25 m/s to 30 m/s.

Talbot et al. (2024) used MPM to model the earthquake induced Lower San Fernando Dam failure. Expanding on the Chowdhury (2018) nonlinear seismic deformation analysis which was unable to capture the large deformation behaviour and post-failure equilibrium cross-section using FDM. For this case study implementation of an adhesion boundary condition was accomplished to reduce the computational cost by limiting the required area to be modelled.

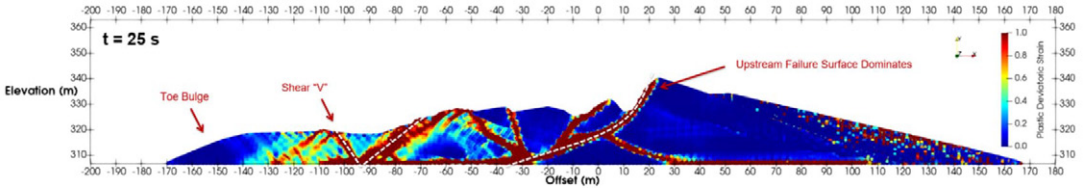

Figure 3: MPM model of Lower San Fernando Dam post-failure (Talbot et al., 2024)

3 INDUSTRY CASE SERIES

3.1 CASE SERIES SUMMARY

A significant number of projects have seen the benefits of improved TDBA studies using MPM methods. The project summary is provided in Table 1. The details described herein are the trends observed by the authors. The project summary includes upstream and downstream-built TSFs. One of the projects considers mud-farming as a dewatering strategy to build a structural zone. Another project involved an Integrated Waste Landform (IWL). Dam height ranges from 20 – 100 m. Commodities include iron ore, coal, gold, manganese, bauxite and red mud. The projects included active, inactive and closed facilities, and those undergoing closure. Most models developed were 2D, although several 3D models are shown. The number of models commissioned per year indicates an increasing trend, which shows a growing interest for this kind of numerical modelling. Multiple models have been successfully submitted to regulators in Australia and overseas. In one case, the MPM model developed was used to update internal TDBA guidelines to inform TDBA studies at the various mine sites in the client's portfolio. Clients are mostly tier-one mining companies. In one case, the TDBA was used to inform a Dam Safety Review (DSR). The MPM model developed for the DSR was instrumental in refining the Consequence Classification Assessment (CCA). A reduction in the CCA risk rating was possible due to the updated TDBA assessment using MPM techniques.

Table 1: Summary of projects for which MPM has been used to improve the outcome of TDBA

Id	Project type	Year	Number of TSFs involved in the TDBA study	Model complexity	Approximate critical cross-section height (m)	Location
1	Inactive Iron Ore Upstream TSF	2019	1	2D	86	Brazil
2	Upstream Coal TSFs	2021	3	2D	15	QLD, Australia
3	Upstream Gold TSF	2021	1	2D	20	NSW, Australia
4	Downstream Manganese TSFs, including active,	2023	5	2D	21	NT, Australia

Id	Project type	Year	Number of TSFs involved in the TDBA study	Model complexity	Approximate critical cross-section height (m)	Location
	inactive and closure construction					
5	Downstream Iron Ore TSF	2023	1	2D	25	WA, Australia
6	Upstream Mud-Farmed Bauxite TSF	2023	1	2D	10	QLD, Australia
7	Active Mining Manganese TSF	2023	1	3D	15	NT, Australia
8	IWL, Gold TSF	2023	1	2D	23	NSW, Australia
9	Closed Bauxite Upstream TSF	2023	1	3D	10	QLD, Australia
10	Inactive Coal Downstream TSF	2024	1	3D	60	QLD, Australia
11	Inactive Iron Ore Upstream TSF	2024	1	3D	86	Brazil
12	Upstream Red Mud	2024	1	2D	90	Spain
13	Downstream Red Mud Closure Construction	2024	1	2D	25	NT, Australia

3.2 CASE STUDIES

This section presents details of key case studies where MPM was used to simulate different tailings dam failure mechanisms. These case studies illustrate the versatility of MPM in capturing complex failure processes that conventional methods may oversimplify or overlook.

3.2.1 The column collapse model

The collapse of a granular column is a well-established experiment in academic publications. The experiment involves releasing a column of granular material by removing its lateral support onto a flat surface. The column fails, and some of its mass crumbles and flows onto the flat surface. In the theoretical abstraction, the instability of the material during collapse is solely driven by the column's self-weight. The research industry has historically focused on understanding how the different aspect ratios of granular columns behave upon collapse (Lube et al. 2004, 2005; Fern & Soga, 2016; Llano-Serna et al., 2016). The aspect ratio is defined as $a = h_0/d_0$, where h_0 and d_0 are the initial column dimensions (height and width, respectively) before the column collapses at $t = 0$. For example, Figure 4 shows the column collapse progression in clayey soil. Llano-Serna et al. (2016) explored aspect ratios of between 0.5 and 10 for normalised time steps of between $t = 0$ (initial conditions) and $t = 4$ (collapsed).

The authors note that the theoretical column collapse problem would better represent tailings dam collapse at very low aspect ratios. Tailings dams are some of the largest man-made structures. In the theoretical column collapse problem context, d_0, tends to infinity; a tailings dam footprint can be several hundred hectares or greater than 1,000 ha for some larger facilities. Despite this key difference between the theoretical column collapse and a real dam breach, similarities exist. A common key geometrical feature can be found between the column collapse with a low aspect ratio of a clayey material in Figure 4 and the post-failure cross-section of the Cadia dam failure in Figure 2.

The final deposited height at the intersection of the profile defined by the collapsed column and the pre-failed geometry is denoted here as h_f. The commonality of this feature is also seen in sandy column collapses, Figure 5. The numerical column collapse of a one-metre-tall loose sand column was compared against experiments. The MPM final run-out was seen to match a laboratory experiment relatively well (Fern and Soga, 2016).

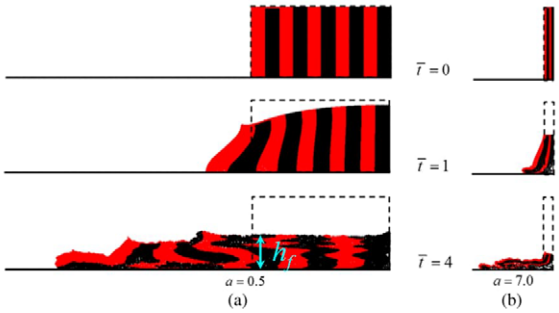

Figure 4: Example of column collapse model using MPM in clayey soil for two aspect ratios. Left: aspect ratio a=0.5, right: a=7 (modified from Llano-Serna et al. 2016)

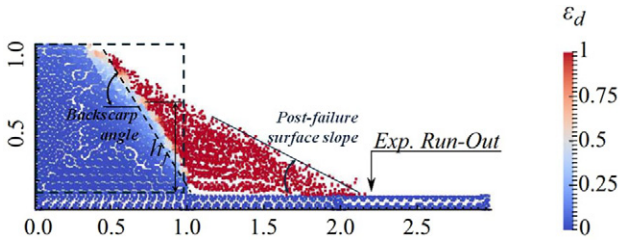

Figure 5: Example of column collapse model using MPM in loose sandy soils with an aspect ratio of one. The colourmap in the background represents the deviatoric strain, ε_d (modified from Fern and Soga, 2016)

MPM modelling allows designers to estimate the slope of downstream deposition angles, see Figure 5. A further added benefit of MPM models is that designers can estimate the interaction between the collapsing material and downstream topographic features. Conventional practices for estimating the post-failure surface slope include the theoretical semi-infinite slope method Seddon (2007) recommended and assuming a factor of safety (FS) equal to one. Adams et al. (2022) propose a method to estimate the so-called stable slope FS. The theoretical semi-infinite slope works well for homogenous deposits where the tailings properties can be assumed to be represented by one characteristic value. For facilities with interbedded tailings that cannot reasonably be considered homogenous, some consultants use the conventional Limit Equilibrium Method (LEM) to estimate the stable slope, which is done by calculating a FS of one, assuming liquefied strengths for the different types of tailings stored in the facility. The theoretical column collapse model has been applied to several TDBA summarised in Table 1. Figure 6 (Top) shows the complex layering and different types of tailings deposited due to the management strategies of a TSF built using mud-farming techniques. In this case, the column's height was approximately 30 m and its width 220 m. Figure 6 (Bottom) shows the final post-collapse geometry calculated using MPM. For this example, the run-out distance was calculated as 270 m, and the post-failure surface was 3.9°.

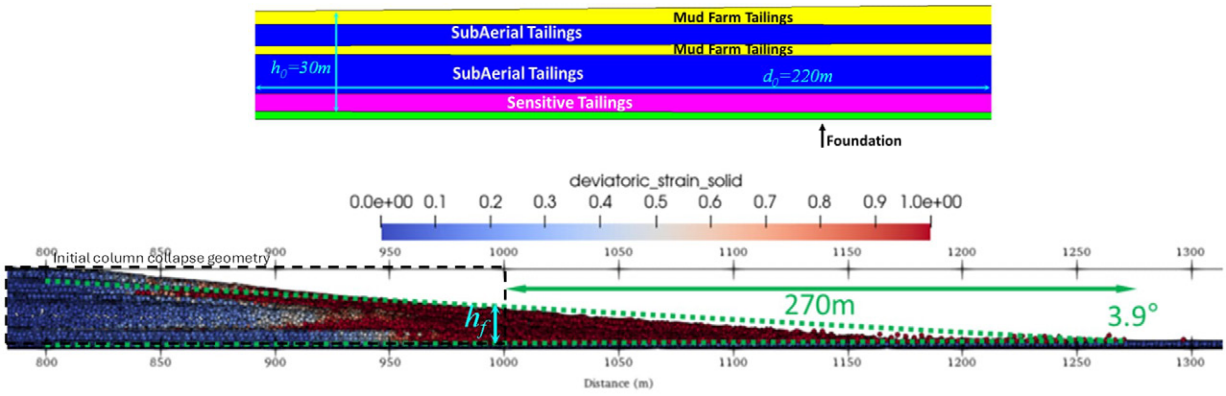

Figure 6: Column collapse modelling applied to TDBA to estimate the deposition angle. Top: initial state, Bottom: final state post-collapse

A summary of the post-failure surface angles calculated for the case studies is provided in Table 2. The results show that the post-failure surface angles vary between 2.7 - 4.2°. A comparison with literature reported by Blight and Fourie (2003) shows alignment between the results presented here and the topographic historical records of previous TSF failures. Specifically, the post-failure surface flattened to a general slope of 2 - 3°, with some portions around the failure scar being

as steep as 10 - 20° (Blight and Fourie, 2003). The close agreement between the post-failure surfaces from MPM models in Table 2 and real failures in Table 3 provides a qualitative validation that supports the credibility of the modelled outputs. Figure 5 shows that MPM also provides insights into the final back scarp angle when the magnitude of deviatoric strain is highlighted. It should be noted that none of the column collapse models summarised herein included a supernatant pond with the focus being conceptual cases 2A and 2B as defined by CDA (2021), which correspond to liquefiable and non-liquefiable tailings without a supernatant pond.

Table 2: Deposition angle calculated using MPM techniques

Id	Project	Model complexity	Post-failure surface slope
2	Upstream Coal TSFs	2D	3°-4°
6	Upstream Mud-Farmed Bauxite TSF	2D	3.9°
8	IWL, Gold TSF	2D	2.7°
11	Inactive Iron Ore Upstream TSF	3D	3.4°-4°
12	Upstream Red Mud	2D	3.9°
13	Downstream Red Mud Closure Construction	2D	4.2°

Table 3: Summary of observed post-failure surface slopes for flow failures (Blight and Fourie, 2003)

Tailings dam	Post-failure surface slope
Bafokeng	4°
Bafokeng	2°
Arcturus	3°
Saaiplas after rain	3°
Saaiplas no rain	2.3°
Saaiplas no rain	3°
Merriespruit flow slide	2°
Merriespruit failure basin	2°

In TDBA, the backscarp angle is projected through the tailings mass beginning at the base of the zone, which would become unconfined during a tailings dam breach. Adams et al. (2022) recommend that the area above the projection of the stable slope angle could liquefy and flow or slump if the lateral confinement is removed. The column collapse model provides estimates of the final backscarp angle and the post-failure surface slope that the authors interpret to be similar or equivalent to Adams' stable slope angle. CDA (2021) and Adams et al. (2022) conservatively recommend that the projection of the final back scarp angle and stable slope has its origin at the intersection between the upstream batter toe and the foundation of the TSF, see the highlighted point in Figure 7. The column collapse model results indicate that the assumption of the location of the origin of the final back scarp can be overly conservative, and the calculated mobilised volume can be greatly overestimated, especially when adopting Adams et al. (2022). This observation is validated when comparing the schematic in Figure 7 with the Cadia post-failure cross-section in Figure 2. These observations are limited to models that do not consider the presence of a supernatant pond.

CDA (2021) recommends using the final back scarp angle to draw a 3D cone of depression to estimate the volume of mobilised tailings when a kinetic model, such as an MPM model, is unavailable. Figure 8 shows the MPM modelled back scarp angle using MPM for the Cadia collapse (Pierce, 2021). The figure shows that the back scarp angle starts more than 100 m upstream from the intersection between the upstream batter toe and the foundation of the TSF. This distance is defined herein as d_b. An alternative to current practices is to refine mobilised volume estimates when a kinetic MPM model is available to estimate the final backscarp angle, d_b, the post-failure slope and h_f. The methodology applies to CDA conceptual cases 2A and 2B. Its application to conceptual cases 1A and 1B (liquefiable and non-liquefiable tailings with a supernatant pond) is possible but should be exercised carefully; such a scenario is discussed in section 3.2.4. The incorporation of measurements from a MPM column collapse model is still considered a conservative estimate because the method disregards the buttressing contribution of the embankment to the dam breach.

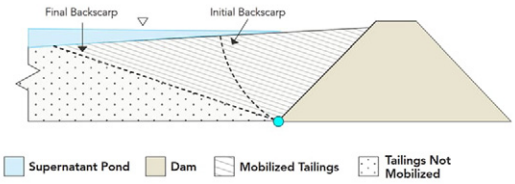

Figure 7: Schematic of the cross-section of the failure surface for a TSF (modified from CDA, 2021)

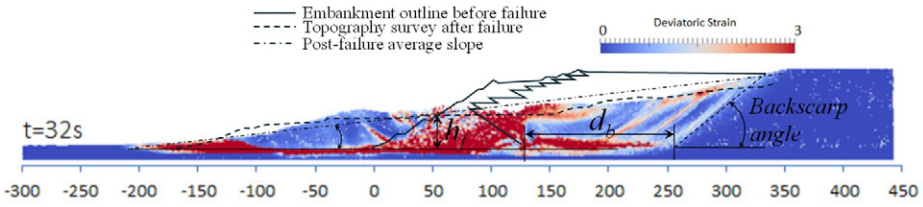

Figure 8: Geometrical features of Cadia MPM model (modified from Pierce, 2021)

3.2.2 Development of hydrographs for input in TDBA hydraulic models

CDA (2021) defines a hydrograph as a graph showing the flow rate (discharge) versus time past a specific point in a river, channel, or conduit carrying flow. The flow rate is typically expressed in cubic metres per second (m^3s^{-1}). Step 7 for undertaking TDBA following CDA involves estimating the breach outflow volumes and breach outflow hydrographs. Key parameters, such as peak flow and outflow define a hydrograph. These parameters can be analysed to assess the severity of the breach, which is influenced by factors like breach size, development time, rheological properties of the released tailings and outflow volume. Hydrographs can also support sensitivity analyses, comparing flood wave scenarios.

A key advantage of using MPM to inform TDBA is that it can be used to develop volume (discharge) vs time plots – the mobilised volume in MPM is an output, not an input variable; it is because the constitutive relationships available in MPM capture the transition between peak and residual strengths, see Zabala and Alonso (2011) and Pierce (2021). The methodology to develop a hydrograph using MPM modelling can be used in subsequent hydraulic modelling, this approach has been employed twice in the project database discussed. The application of this approach corresponds to Project three and Project 11 in Table 1. Project three is a 2D application, and Project 11 is a 3D application. Only Project three is briefly described.

For Project three the TSF was 20 m high; the critical cross section is shown in Figure 9. It comprised one starter embankment and five subsequent upstream raises. The critical failure mode assessed was static liquefaction of the tailings. The CDA conceptual case was classified as 2A. The footprint of the TSF is shaped like a pentagon; see Figure 10. For this study, it was requested by stakeholders that the failure of the entire wall, highlighted in red in Figure 10, was considered. Due to the extension of the wall in the axis perpendicular to the page, a 2D analysis was considered appropriate for developing a hydrograph.

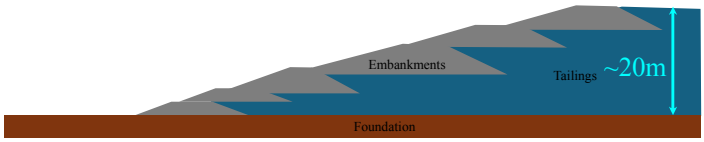

Figure 9: Critical cross-section of the embankment considered critical for TDBA scenario

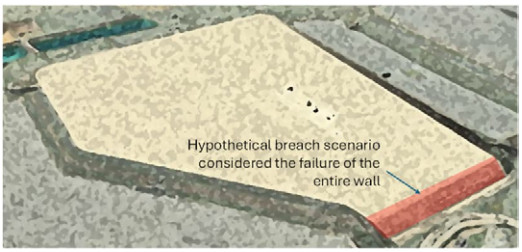

Figure 10: Panoramic view of a TSF for which TDBA was undertaken using MPM techniques, the vertical scale has been exaggerated

The MPM mesh adopted for this case study is presented in Figure 11. The MPM engine Anura was used to solve this model. Multiple conservative simplifications were considered: i) the contribution of the embankments to the collapse of the TSF was ignored, ii) a boundary condition consisting of lateral support on the upstream batters was imposed at t=0, the location of the lateral support is sketched in yellow in, iii) initial stresses were developed while the lateral support was active by imposing gravity loading in a quasi-static manner, iv) the tailings were assigned liquefied properties – a conservative 95th percentile liquefied undrained shear strength ratio (LUSSR) which resulted in a value of 0.032. An excavation boundary condition was defined at the toe of the TSF (green box in Figure 11), this boundary condition removed tailings material points that displaced beyond the TSF toe. This last boundary condition is conservative because it ignores the buttressing effect of the tailings that would otherwise deposit downstream of the failed wall. Removing the lateral support activated the TSF breach, this approach assumes a trigger. The bottom and lateral boundary conditions applied in this case study were consistent with those used in conventional geotechnical numerical modelling. It should be noted that Figure 11 shows the portion of the model near the embankment toe only. The entire model considered several hundred metres horizontally to capture the real TSF geometry.

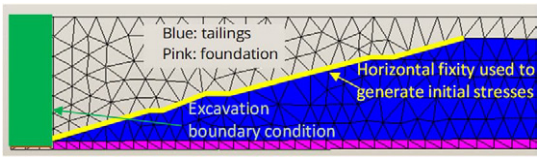

Figure 11: MPM mesh and boundary conditions required for TDBA modelling

In MPM, each material point has a mass associated with it. Building a flow rate vs time plot is ubiquitous because most MPM models are explicit in time. Figure 12 shows the plot of tailings (discharge expressed in tons per second) vs time (in seconds) obtained using MPM. The orange dots correspond to actual MPM measurements, and the red line is the moving average with a period calculated using four data points. The data was utilised to develop a series of hydrographs for subsequent inundation modelling.

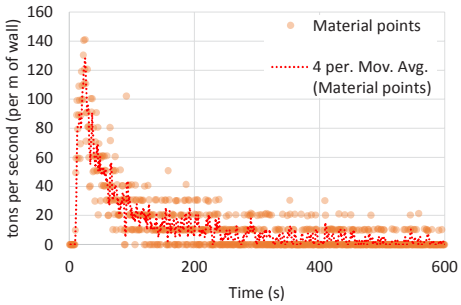

Figure 12: Calculated hydrograph using MPM

3.2.3 Cascading failure mode

A cascading failure scenario was analysed for a turkey nest TSF structure without external catchments, where the primary risk involved the potential for failure of the upstream facility to trigger overtopping of the downstream facility. The upstream facility would release a mass of tailings into the decant pond of the downstream facility, causing a significant wave. This wave could result in overtopping of the downstream dam, leading to a loss of contaminants. MPM was used in the TDBA of the upstream TSF. The application of this method corresponds to Project eight in Table 1. The upstream facility was inactive, with pumping infrastructure installed to manage rainwater run-off – a no decant pond scenario was assumed; the downstream facility was active with a decant pond. The analysis focused on quantifying the key parameters driving wave generation to assess the consequence and impact of this cascading failure. Heller et al. (2009) studied the governing parameters of landslide-generated impulse waves in reservoirs; the key parameters are presented in Figure 13.

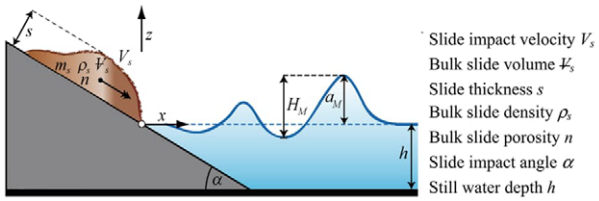

Figure 13: Sketch defining the governing parameters on impulse wave generation and the most important wave parameters (modified from Heller et al. 2009)

Inspection of Figure 13 reveals that most parameters could reasonably be estimated using topographic surveys and conventional geotechnical studies. Slide impact velocity in particular, is not usually reported in geotechnical studies. MPM was used in this case study to inform slide impact velocity.

The initial stress state was computed using FLAC. The stresses were later imported into MPMPUC-Rio. The following assumptions and simplifications were considered: i) The tailings were assigned a LUSSR of 0.07, ii) the buttressing effect of the decant pond in the downstream tailings was ignored, iii) the groundwater level in the tailings downstream was defined at 1 m below the tailings level – this assumption was needed because the MPM model did show numerical instabilities when tailings downstream were allowed to generate pore pressures near the surface. Figure 14 shows the defined regions. Figure 15 shows the final deformed dam calculated with MPM with the deviatoric strain colourmap highlighted. The final maximum horizontal displacement was expected to be approximately 2 metres. A deviatoric strain plot is useful because it reveals the location of failure surfaces when the deviatoric strain reaches unity (shown in red). Figure 16 shows the velocity vs time plot, showing that peak velocity occurs approximately ten seconds after the event is triggered and reaches maximum velocity of 1.8 m/s. The results show that after 30 seconds, the dam failure stabilised. The intensity/darkness of the orange shading inside the plot in Figure 16 indicates the number of material points for which the same velocity was recorded at each time step.

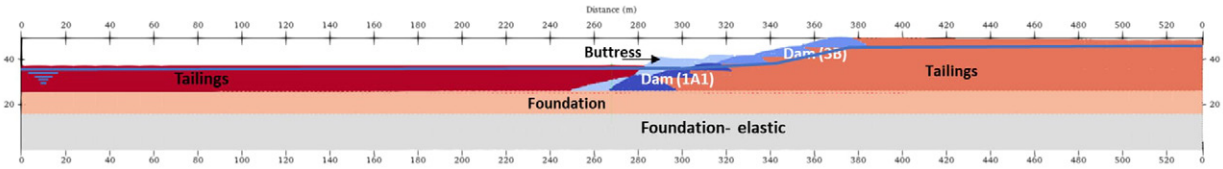

Figure 14: Cascading failure mode case study, cross section showing defined regions

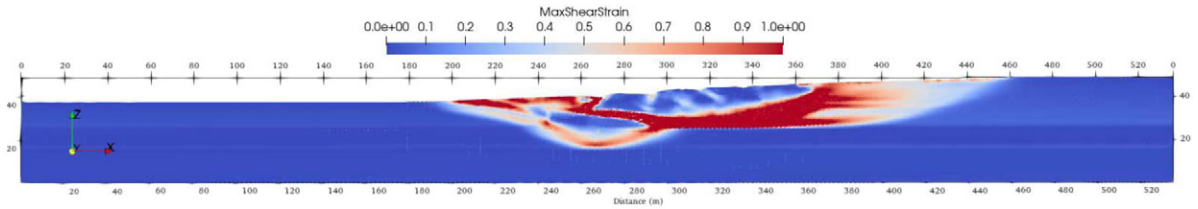

Figure 15: Final deviatoric strain colourmap with red regions indicating the position of a complex failure mechanism during a hypothetical dam breach scenario

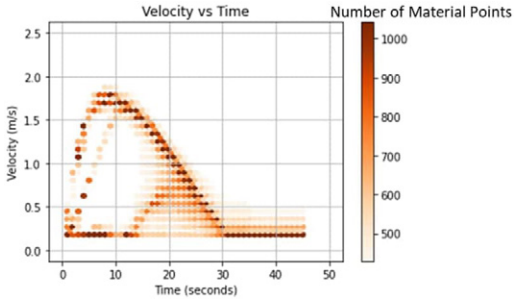

Figure 16: Velocity vs time plot during the hypothetical dam breach scenario

3.2.4 Dam breach of a dewatered/mud-farmed TSF

The following is an example of when MPM was utilised to analyse breach scenarios for an upstream TSF in Australia. A structural zone in the TSF was built using mud-farmed tailings. Anura was the MPM engine used to solve this case study. This summary corresponds to Project six in Table 1. Seyedan et al. (2024) documented a detailed description of the approach for this case study, including boundary conditions and material parameters. The mud-farmed tailings were modelled with a post-peak frictional angle of 25° and the subaerial deposited tailings with a LUSSR of 0.13.

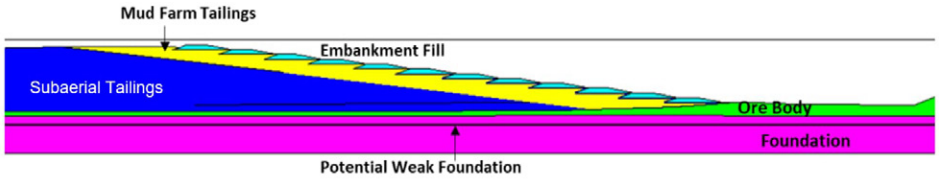

Figure 17:Typical section in the upstream mud-farmed TSF showing the structural zone in yellow and the potential weak foundation in black

A potentially weak layer was identified in the foundation. MPM was then used to investigate credible failure modes, like potential dam breaches due to foundation deterioration. The investigation applied residual material strength that could lead to dam instability. Fern and Soga (2016) demonstrated how this assumption results in conservative estimates. MPM modelling involved critical cross-sections at various stages of the TSF's lifecycle. Figure 18 displays the horizontal (X) and vertical displacement (Y) colourmap (in metres) for one of the critical cross-sections. The results indicates that the maximum horizontal displacement is 45 m, with the displacement extending approximately 60 m upstream of the TSF. The results also indicate a 10 m loss of freeboard at the crest location and shows negligible loss of freeboard at approximately 60 m upstream from the dam crest. This information was relevant for determining pond operational levels. Pond size is crucial for defining the risk profile and avoiding a release during a potential breach. This is an example of the effective use of MPM modelling in facilities with existing ponds – see CDA (2021) conceptual cases.

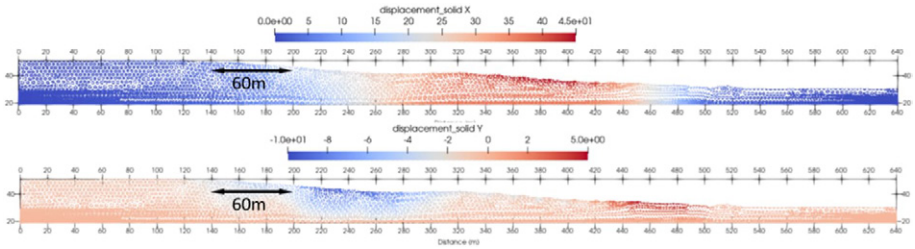

Figure 18: Horizontal and vertical displacements for the critical cross-sections in the mud-farmed TSF

3.2.5 3D MPM modelling

In certain cases, 2D models may not represent field conditions due to complex geometry, non-uniform loading conditions, etc. This section highlights two examples where 3D MPM models were used.

3D MPM modelling – Case A

An MPM model was developed as part of a risk reduction study on a TSF built using the downstream method. The dam is 60 m in height, constructed on bedrock using spoil material—a mixture of silty clay and gravel—the tailings were predominantly comprised of fine material exhibiting medium to high plasticity. The TSF was an inactive facility without a pond. This project corresponds to Project ten in Table 1. The initial stresses for this model were solved using FLAC3D and the run-out process was solved using MPMPUC-Rio. The embankment dam materials were modelled as dilative materials that would reach post-peak friction angles of between 18 - 20° during a hypothetical dam breach. Figure 19 (left) shows a panoramic view of the facility in the FLAC environment. The results from the runout analysis at the end of the simulation and after all materials had settled are shown in Figure 19 (right). The expected maximum run-out was 100 m. A key outcome was that the results predicted no loss of tailings containment should post-peak strengths develop.

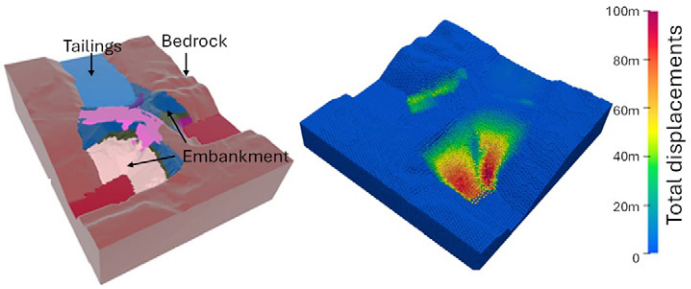

Figure 19: Left: FLAC model, right: MPM model displacements after failure

3D MPM modelling - Case B

An analysis was conducted to assess the potential impacts of a TSF failure on nearby infrastructure (i.e. road and settlement). The TSF was constructed using the upstream method, with a 8 m high starter embankment and a single raise of 2 m, for a total TSF height of 10 m. MPMPUC-Rio was the solver used. The case study is Project nine in Table 1. Following recommendations from CDA (2021), a sensitivity analysis was conducted using hypothetical dam breach scenarios, including realistic and pessimistic scenarios.

- The realistic scenario used mean strength values, representing the most likely condition.
- The pessimistic scenario assumed lower strength bound values to simulate worst-case scenario conditions.

Figure 20 shows the inundation map from the pessimistic scenario (tailings LUSSR of 0.04). In this scenario the embankments were assumed to have the same strength as tailings due to lack of geotechnical information. The TSF breach released impounded material towards the nearby settlement and reached the nearby road.

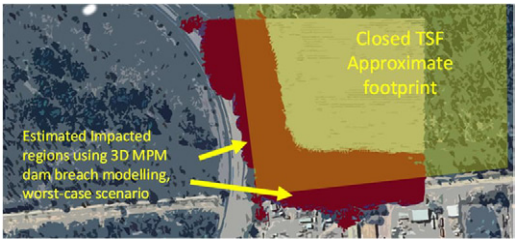

Figure 20: Inundation map of impacted regions using 3D MPM dam breach modelling for a worst-case scenario

4 DISCUSSION

MPM is an additional tool that TSF operators and design engineers can use to improve the accuracy of TDBA under certain conditions. The models presented are varied to showcase the uses of MPM, they have been included in TDBA studies for clients, including regulators in Australia and overseas. One usage that reoccurs throughout is that of emergency response planning, which benefits from the more realistic spatial and temporal results produced by MPM. The subsequent discussion includes recommendations to aid in optimising MPM modelling for the credibility of FMEAs and consequence modelling; it is supported by the results in the project database summarised in Table 1.

4.1 PARAMETERS AND MODELLING APPROACH

Hydraulic modelling or computational fluid mechanics (CFD) software like DAN3D, MADflow, FLO-2D, FLOW-3D or HEC-RAS is the most common approach to model dam breaches. The most common constitutive models in these software packages are Voellmy, Quadratic or Bingham rheology. The combination of these software packages with these constitutive relationships is a powerful tool when modelling water floods and mud floods. However, there are significant uncertainties in some of the results they can provide when modelling non-Newtonian fluid. Ghahramani et al. (2022) demonstrated one of the main uncertainties, in that irrespective of the constitutive modelling or software used, multiple sets of rheological parameters may produce very similar output results (i.e. the solution may not be unique, or there are infinite solutions). Additionally, input parameter combinations are non-transferable between models or software packages (e.g., the same viscosity and yield stress will likely produce very different outcomes when using different software packages, even when the same rheological constitutive relationship is used). Differences of several orders of magnitude in viscosity to reach the same outcome were noted by Ghahramani et al. (2022). Ghahramani et al. (2022) also reported inconsistent back-calculated viscosities when compared with independently measured rheological properties of a tailings parameter database.

MPM can be used to solve models using constitutive relationships well known by tailings practitioners, including failure criteria like Mohr-Coulomb and the elasto-plastic constitutive models Cam-Clay and Nor-Sand. Fern and Soga (2016) show how different constitutive relationships solved with the same MPM engine can provide comparable results, results which were then validated with a laboratory experiment (Figure 21). The black arrow in each figure refers to the runout distance from the laboratory experiment. These results show that MPM can provide consistency across various constitutive relationships when adopted with equivalent material parameters (see Table 4).

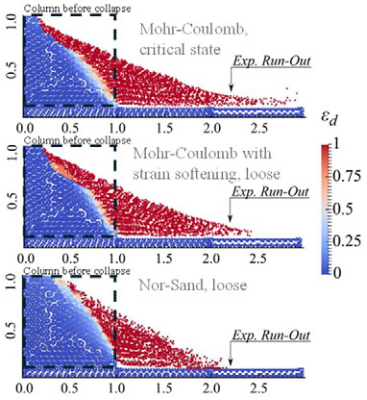

Figure 21: MPM results of simulations of a loose sand squared column of 1 m. The colourmap represents the deviatoric strain (modified from Fern and Soga, 2016)

A column collapse using two different MPM engines was modelled using Anura and MPMPUC-Rio. The material parameters for both models were kept constant to verify the transferability of parameters across different MPM implementations. The results in **Figure 22** were obtained with the same set of parameters used in different MPM engines to provide comparable results. This parameter transferability across different software packages is a feature that the most widely used software for TDBA lacks; see Ghahramani et al. (2022). The model comparison in **Figure 22** also exemplifies the evolution in computational efficiency; the mesh size is much finer in the 2020 MPMPUC-Rio than in the 2016 Anura model. A finer mesh is generally desirable because it captures more detail, such as the development of stress/strain. The capacity to develop finer meshes also translates into the capacity to solve larger models (with coarser meshes), such as those needed in TDBA studies for TSF structures.

Table 4: Summary of key strength parameters adopted by Fern and Soga (2016)

Constitutive model	Strength material parameter
Mohr-Coulomb at critical states	ϕ'=33°
Mohr-Coulomb with strain softening	ϕ'_{peak}=39° $\phi'_{residual}$=33°
Nor-Sand	M_{tc}=1.33 (ϕ'_{cv}=33°)

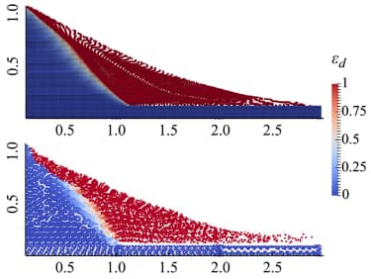

Figure 22: Comparison of the runout distances and deviatoric stress distribution for a 1 m column with an effective friction angle of 33°, top: MPMPUC-Rio, bottom: Anura3D (Soga and Fern, 2016)

4.2 SOLIDS CONTENT

CDA (2021) classifies the types of breach outflows based on the tailings solids contents: a) water flood, b) mud flood, c) mud flow, d) flows slide slumping. **Figure 23** illustrates the relationship between the concentration of solids and CDA tailings breach outflow types. The blue stars in **Figure 23** show the location within the plot of some past successful projects where MPM was used. Mud flow and Flow slide slumping (highlighted with the light blue arrows at Cv ~ 0.5) show the recommended region of tailings solids content that are capable of being modelled using MPM. It is the authors' experience that MPM modelling is most useful for emergency planning, credible failure modes and consequences involving flow slide or slumping scenarios that could lead to catastrophic damage downstream. The kind of MPM modelling presented here, derived from soil mechanics principles, could be extended to model low solids concentration

mud flows or mud floods. However, this would require rheological models to be implemented in the MPM solver (the authors note that versions of Anura and CB-Geo include Bingham rheology implementations). Solving rheology with MPM is computationally expensive, and for lower solids concentration, it is recommended to adopt the numerical techniques highlighted by CDA.

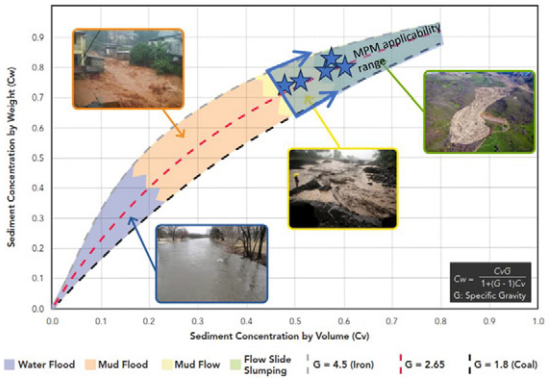

Figure 23: Flow types as a function of solids concentration, modified from CDA (2021)

4.3 RHEOLOGICAL BEHAVIOUR

Rheology describes the interrelation between stresses, strains and time-dependent behaviour. The yield stress is a key parameter measured for rheological studies to inform TDBA. Adams et al. (2018) described how the tailings transition from a slurry to a paste and then soil as the yield stress increases, developing four flowability zones. MPM modelling has been used to model tailings classified between the transition and the flowable zones. Seyedan et al. (2024) have shown examples of applying MPM models for TDBA of mud-farmed (i.e. a dewatering tailings technique that results in high solids concentrations) TSFs whereby mud-farmed tailings are classified as either not flowable or within the transition zone associated with potential slide flow or slumping scenarios. The applicability of MPM is maximised when applied to facilities with not flowable or transition tailings, as those described by Adams et al. (2018).

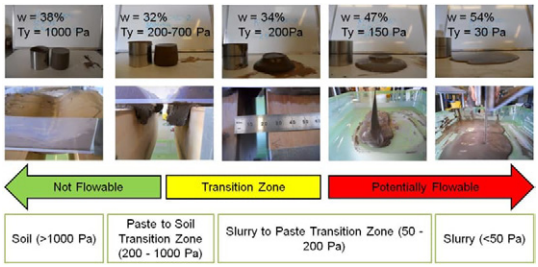

Figure 24: Tailings rheology: solids to slurry continuum (Adams et al., 2018)

4.4 TDBA CASES

CDA defined four conceptual TDBA cases (1A, 2A, 1B and 2B). The cases combine the potential for tailings runout due to flow liquefaction and the presence of a supernatant pond. Provided that tailings within a facility are within the boundaries described in Sections 4.1 and 4.2, MPM modelling for tailings dam breach estimates are applicable for cases 2A and 2B (which also encompasses a significant number of inactive and closed TSFs). MPM modelling is also appropriate for Cases 1A and 1B if tailings are characterised within the boundaries defined by solids content and rheological behaviour discussed herein, and no potential loss of pond containment can be demonstrated. For example, the results from the mud-farmed TSF shown in the study suggested that MPM could simulate the effects of a flow slide slump, provided pond containment is maintained at safe distances—typically 60 m from the dam crest for that TSF. MPM modelling may be used to estimate the release volume of solids for cases 2A and 2B, involving release of pond containment providing the releases of supernatant water and tailings are expected to occur in independent phases. MPM can inform dam breach, uncontrolled release of reservoir (URR), and rate of breach/URR for a Case 1A type of facility. The assessment to evaluate the potential loss of containment must be undertaken on a case-by-case basis with appropriate numerical modelling and assumptions. No rule of thumb can be established for complex scenarios.

4.5 VOLUME ESTIMATES

Ghahramani et al. (2024) back analysed 11 well-documented historical tailings breaches and found that for approximately 80% of the historical cases, the inundation area was the most sensitive to the total released tailings volume. Therefore, estimating the total released tailings volume is key to undertaking a TDBA. Empirical methods to estimate mobilised volume such as Rico et al. (2008), Rourke and Luppnow (2015), Concha Larrauri and Lall (2018) or Ghahramani et al. (2020) can have uncertainties of more than one order of magnitude, making its application to estimate mobilised tailings volume controversial (i.e. it can drive easily non-credible results) because mobilised volume estimates often drive the highest sensitivity to results, see Ghahramani et al. (2022, 2024).

CDA (2021) advocates the use of the cone of depression method when kinetic analysis such as MPM are not available. The results shown illustrate the potential to refine the cone of depression method by incorporating the back scarp angle, the post-failure surface slope and parameter h_f measured in column collapses. Refining the total released volume estimate with geotechnical parameters such as post-peak frictional angles or LUSSR in the true TSF geometry to estimate hydrographs.

More complex models like Nor-Sand, which can replicate the peak and liquefied strength, are alternatives suitable to improve mobilised volume estimated, but more difficult to readily implement due to the required information and budget to undertake such assessments. Fern and Soga (2016) present examples of Nor-Sand applications in the academic MPM column collapse context.

Strategies i - vii are available to practitioners looking to apply MPM to refine released tailings volume estimates. The strategies are shown and explained in order of complexity, starting with the simplest methodologies and proceeding to the most difficult. Strategies i and ii may be built up with complexity to include layering with each layer having distinct properties. These modelling strategies have seen great acceptance among stakeholders undertaking TDBA studies and have been used in the case series presented.

i) Column collapse to estimate post-failure surface slopes or backscarp angles for subsequent cone of depression volume estimates
ii) Column collapse to estimate post-failure surface slopes or backscarp angles, d_b and h_f for subsequent cone of depression volume estimates
iii) Collapse of the TSF cross-section with simplifying assumptions such as assigning the same LUSSR to tailings and embankment materials and an excavation boundary at the toe to quantify a hydrograph for subsequent hydraulic modelling for the run-out phase
iv) Collapse of the TSF cross-section with simplifying assumptions such as assigning the same LUSSR to tailings and embankment materials and modelling the run-out and deposition using MPM
v) Collapse of the TSF cross-section assigning LUSSR to tailings and residual strengths for embankment materials (this alternative has seen great acceptance between clients and engineers of record)
vi) Collapse of the TSF geometry in 3D with simplifying assumptions such as assigning the same LUSSR to tailings and embankment materials
vii) Collapse of the TSF geometry in 3D assigning LUSSR to tailings and residual strengths for embankment materials.

It is the authors view that with continuous market penetration of MPM in the tailings industry, we anticipate that models encompassing breach/failure triggering will begin to be utilised. Defined here as reproduction of a failure event that captures the transition from peak to residual/liquefied strengths due to an imposed loading condition such as seismic loading, increase in groundwater levels, lateral extrusion, creep settlement, etc. The development of hydrographs will increase as sufficient computational power becomes more readily available, enabling modelling of the run-out and tailings deposition. Specific scenarios where this may be applied include:

i) Breach/failure triggering of the TSF geometry in 3D using strain softening models such as Mohr-Coulomb with strain softening, Nor-Sand or similar, to replicate the peak to liquefied/residual state transition; see Arenas and Pereira (2024) and Saeedi et al. (2024)
ii) Breach/failure triggering of the TSF geometry in 3D using strain softening models to replicate the peak to liquefied/residual state transition and to model the potential breach width
iii) incorporation of ponding water on top of tailings to capture overtopping and embankment erosion. Some academic examples using Anura already exist; see Yang et al. (2019).

5 CONCLUSIONS

MPM as a modelling technique has been introduced and discussed as a tool for tailings practitioners in the industry to address some of the complex challenges faced when assessing risk. The development of MPM and some of available packages were highlighted. In addition to four examples of forensic studies that have employed MPM, six industry

projects (four 2D and two 3D) were briefly described, highlighting examples where MPMs usage was able to contribute to the outcomes of the project. The advantages of utilising industry standard geotechnical models within MPM are significant, while the computational effort and required expertise are the main drawbacks. Incorporating MPM into breach assessments and the various scenarios where this might be beneficial were highlighted as this aspect features heavily in most risk assessments.

Overall MPM represents a significant step towards modelling realistic scenarios that involve large strain, scenarios that we within the industry were previously not able to model efficiently. By closing the gap between modelled behaviour and actual behaviour the credibility of a failure mode can be investigated with more rigour and confidence. This interrogation of a failure mode occurring is critical for risk management of tailings facilities and feeds into FMEAs, emergency planning, category classification, breach assessments and much more. It is hoped that this paper will be beneficial to practitioners seeking to employ MPM within their projects going forward as we continue to move towards the GISTM goal of 'zero harm to people and the environment with zero tolerance for human fatality.'

CRediT authorship contribution statement

Marcelo Llano-Serna: Writing - original draft. **Scott Lines:** Writing – review and editing. **Nicolas Pereira:** Writing - original draft. **Seyedmohammadjavad Seyedan:** Writing - original draft. **Sudheer Prabhu:** Writing – review and editing. **Mike Liu:** Writing – review and editing.

6 REFERENCES

Adams, A., Brouwer, K., Robertson, P.K. and Martin, V. (2022). Evaluation of Tailings Behaviour for Dam Breaches. *Proceedings of Tailings and Mine Waste 2022*.

Arenas, A., and Pereira, N. (2024). Feijão Dam I 3D Numerical Simulation: A Comprehensive Approach, from Triggering to Dam Breach. *Proceedings of Tailings and Mine Waste 2024*.

Anura3D MPM Research Community (2025), *Anura3D Tutorial Manual version v2025*

Australian National Committee on Large Dams (ANCOLD) (2022). *Guidelines on Risk Assessment*.

Bardenhagen, S. G., & Kober, E. M. (2004). The generalized interpolation material point method. *Computer Modeling in Engineering and Sciences*, *5*(6), 477-496.

Blight, G. E., & Fourie, A. B. (2003, May). A review of catastrophic flow failures of deposits of mine waste and municipal refuse. In *International Workshop on occurrence and mechanisms of flow in natural slopes and earthfills*.

Canadian Dam Association (CDA) (2007). *Dam Safety Guidelines*

Canadian Dam Association (CDA) (2021). *Technical Bulletin: Tailings Dam Breach Analysis*

Chowdhury, K. H. (2018). Evaluation of the State of Practice Regarding Nonlinear Seismic Deformation Analyses of Embankment Dams Subject to Soil Liquefaction Based on Case Histories. University of California, Berkeley.

Concha Larrauri, P., & Lall, U. (2018). Tailings dams failures: updated statistical model for discharge volume and runout. *Environments*, *5*(2), 28.

Fern, E. J., & Soga, K. (2016). The role of constitutive models in MPM simulations of granular column collapses. *Acta Geotechnica*, *11*(3), 659-678.

Fernández, F, (2020). Modelagem numérica de problemas geotécnicos de grandes deformações mediante o método do ponto material. Pontifícia Universidade Católica de Rio de Janeiro, PUC-Rio, Rio de Janeiro, Brasil.

Global Tailings Review GTR (2020). *Global Industry Standard on Tailings Management (GISTM)*.

Ghahramani, N., Adria, D. A., Rana, N. M., Llano-Serna, M., McDougall, S., Evans, S. G., & Take, W. A. (2024). Analysis of Uncertainty and Sensitivity in Tailings Dam Breach-Runout Numerical Modelling. *Mine Water and the Environment*, *43*(1), 87-103.

Ghahramani, N., Chen, H. J., Clohan, D., Liu, S., Llano-Serna, M., Rana, N. M., ... & Take, W. A. (2022). A benchmarking study of four numerical runout models for the simulation of tailings flows. *Science of the Total Environment*, *827*, 154245.

Ghahramani, N., Mitchell, A., Rana, N. M., McDougall, S., Evans, S. G., & Take, W. A. (2020). Tailings-flow runout analysis: examining the applicability of a semi-physical area–volume relationship using a novel database. *Natural Hazards and Earth System Sciences*, *20*(12), 3425-3438.

Heller, V., Hager, W. H., & Minor, H. E. (2009). Landslide generated impulse waves in reservoirs: Basics and computation. *VAW-Mitteilungen*, *211*.

International Commission on Large Dams (ICOLD) (2022) *Bulletin 194 - Tailings Dam Safety*

Kumar, K., Salmond, J., Kularathna, S., Wilkes, C., Tjung, E., Biscontin, G., & Soga, K. (2019). Scalable and modular material point method for large scale simulations. In *2nd International Conference on the Material Point Method*. Cambridge, UK.

Llano-Serna, M. A., Farias, M. M., & Pedroso, D. M. (2016). An assessment of the material point method for modelling large scale run-out processes in landslides. *Landslides*, *13*, 1057-1066.

Llano-Serna, M. (2023). On the consequences of getting dam breach analysis wrong. *Friction. https://www.friction.news/news/on-the-consequences-of-getting-dam-breach-analysis-wrong*

Llano-Serna, M. A., Seyedan M.J., Hazard, J. (2024) A paradigm shift in geotechnical risk management: tailings dam breach analysis using material point method techniques for inactive and closed tailings storage facilities. *Australian Centre for Geomechanics.* https://acg.uwa.edu.au/2024/12/04/mine-closure-article-by-marcelo-llano-red-earth-engineering-a-geosyntec-company-mj-seyedan-geosyntec-consultants-jim-hazzard-itasca-consulting-group/

Lube, G., Huppert, H. E., Sparks, R. S. J., & Hallworth, M. A. (2004). Axisymmetric collapses of granular columns. *Journal of Fluid Mechanics*, *508*, 175-199.

Lube, G., Huppert, H. E., Sparks, R. S. J., & Freundt, A. (2005). Collapses of two-dimensional granular columns. *Physical Review E—Statistical, Nonlinear, and Soft Matter Physics*, *72*(4), 041301.

Martens, S. and Kupper, A. (2024). Credible Failure Modes: considerations for assessment and application. *Proceedings of Tailings and Mine Waste 2024*, Colorado.

National Academies of Science, Engineering and Medicine (NASEM) (2021). *State of the Art and Practice in the Assessment of Earthquake-Induced Soil Liquefaction and its Consequences*

Pierce, I. (2021). *Applying the Material Point Method to Identify Key Factors Controlling Runout of the Cadia Tailings Dam Failure of 2018* (Dissertation, Virginia Tech).

Purvance, M., & Coetzee, C. (2024). MPAC–Material Point Analysis of Continua. *Applied Numerical Modeling in Geomechanics -2024*

Robertson, P.K., de Melo, L., Williams, D.J., & Wilson, G.W. (2019). *Report of the expert panel on the technical causes of the failure of Feijão Dam I*, from http://www.b1technicalinvestigation.com/

Rico, M., Benito, G., & Diez-Herrero, A. (2008). Floods from tailings dam failures. *Journal of hazardous materials*, *154*(1-3), 79-87.

Rourke, H., & Luppnow, D. (2015). The risks of excess water on tailings facilities and its application to dam-break studies. *Tailings and Mine Waste Management for the 21st Century*, 225-230.

Saeedi, A., Martinelli, M., & Simms, P. (2024). Multi-model analyses of tailings impoundment failure and runout: part iii. *Proceedings of Tailings and Mine Waste 2024*.

Sołowski, W. T., Berzins, M., Coombs, W. M., Guilkey, J. E., Möller, M., Tran, Q. A., Adibaskoro, T., Seyedan, M., Tielen, R., & Soga, K. (2021). Material point method: overview and challenges ahead. In *Advances in Applied Mechanics*, *54*, 113-204.

Sulsky, D., Zhou, S.J. and Schreyer, H.L., 1995. Application of a particle-in-cell method to solid mechanics. *Computer physics communications*, *87*(1-2), pp.236-252.

Sulsky, D., Chen, Z. and Schreyer, H.L., 1994. A particle method for history-dependent materials. *Computer methods in applied mechanics and engineering*, *118*(1-2), pp.179-196.

Seddon, K. D. (2007, March). Post-liquefaction stability of thickened tailings beaches. In *Proceedings of the Tenth International Seminar on Paste and Thickened Tailings, Australian Centre for Geomechanics, Perth* (pp. 395-406).

Sadeghirad, A., Brannon, R. M., & Burghardt, J. (2011). A convected particle domain interpolation technique to extend applicability of the material point method for problems involving massive deformations. *International Journal for numerical methods in Engineering*, *86*(12), 1435-1456.

Seyedan, S., Arenas, A., & Llano-Serna, M. (2024). Advances in dam breach analysis appropriate for dewatered tailings storage facilities. In *Paste 2024: Proceedings of the 26th International Conference on Paste, Thickened and Filtered Tailings* (pp. 247-256). Australian Centre for Geomechanics.

Small, A., Küpper, A., Johndrow, T. and Al-Mamun, M.M. (2023). Credible Failure Modes: Summary of 2021 and 2023 Workshops. *Proceedings of Tailings and Mine Waste 2023*, Vancouver, 1245-1255.

Talbot, L. E., Given, J., Tjung, E. Y., Liang, Y., Chowdhury, K., Seed, R., & Soga, K. (2024). Modeling large-deformation features of the Lower San Fernando Dam failure with the Material Point Method. Computers and Geotechnics, 165, 105881.

United States Society on Dams (USSD) (2022). *Analysis of Seismic Deformations of Embankment Dams.*

Wallstedt, P. C., & Guilkey, J. E. (2008). An evaluation of explicit time integration schemes for use with the generalized interpolation material point method. *Journal of Computational Physics*, *227*(22), 9628-9642.

Yang, Y. S., Yang, T. T., Qiu, L. C., & Han, Y. (2019). Simulating the overtopping failure of homogeneous embankment by a Double-Point Two-Phase MPM. *Water*, *11*(8), 1636.

Zabala, F., & Alonso, E. E. (2011). Progressive failure of Aznalcóllar dam using the material point method. *Géotechnique*, *61*(9), 795-808.